Journal of
Composites Science

MDPI

Article

Preparation and Mechanical Properties of Graphene/Carbon Fiber-Reinforced Hierarchical Polymer Composites

Jose M. Vázquez-Moreno [1], Ruben Sánchez-Hidalgo [2], Estela Sanz-Horcajo [1], Jaime Viña [3], Raquel Verdejo [1] and Miguel A. López-Manchado [1,*]

1 Institute of Polymer Science and Technology (ICTP-CSIC), C/ Juan de la Cierva 3, 28006 Madrid, Spain; chemavm78@gmail.com (J.M.V.-M.); estela.sanz.horcajo@upm.es (E.S.-H.); rverdejo@ictp.csic.es (R.V.)
2 Instituto Nacional del Carbón, INCAR-CSIC, C/ Francisco Pintado Fe 26, 33011 Oviedo, Spain; rubensanchezhidalgo@gmail.com
3 Department of Materials and Metallurgical Engineering, University of Oviedo, Edificio Departamental Este, Campus de Viesques, 33203 Gijón, Spain; jaure@uniovi.es
* Correspondence: lmanchado@ictp.csic.es; Tel.: +34-915-622-900

Received: 22 February 2019; Accepted: 22 March 2019; Published: 25 March 2019

Abstract: Conventional carbon fiber-reinforced plastics (CFRP) have extensively been used as structural elements in a myriad of sectors due to their superior mechanical properties, low weight and ease of processing. However, the relatively weak compression and interlaminar properties of these composites limit their applications. Interest is, therefore, growing in the development of hierarchical or multiscale composites, in which, a nanoscale filler reinforcement is utilized to alleviate the existing limitations associated with the matrix-dominated properties. In this work, the fabrication and characterization of hierarchical composites are analyzed through the inclusion of graphene to conventional CFRP by vacuum-assisted resin infusion molding.

Keywords: composite; hierarchical; carbon fiber; graphene

1. Introduction

Conventional fiber-reinforced plastics (FRP) exhibit an excellent specific strength and stiffness, impact resistance, low weight, durability, and good chemical and environmental resistance. These characteristics have made them one of the most important materials for many structural applications, including aeronautical, automotive, renewable energy, sports equipment, construction materials, etc. [1–7]. Although they present excellent in-plane properties, the through-thickness behavior of FRP is weak, in particular, the interlaminar delamination resistance. Interlaminar delamination is a major challenge in the design of composite structures [8]. The main factor causing delamination in laminates is the weak fiber/matrix interface and the brittle nature of the resins. Several approaches have been explored to improve the interfacial adhesion, such as Z-pinning, stitching and braiding, but these processes are complex and expensive, and also tend to reduce the in-plane laminate performances, as they damage the primary fibers [9]. Another alternative is to increase the surface area and reactivity of the fibers through surface modifications, plasma treatment, thermal modification or chemical functionalization, but the increase in properties has usually been modest [10–13]. In the last decade, there has been growing interest in the development of hierarchical composite materials, in which a nanometer-scale particle is incorporated into the conventional fiber composite material [14–16]. So far, the main nanoparticle used has been multi-walled carbon nanotubes (MWCNTs), because they have good mechanical properties and because their cost is lower than single-wall carbon nanotubes (SWCNTs). CNTs have been incorporated following two main procedures: (i) CNTs have been directly

mixed with the resin for subsequent infusion into the laminates, or (ii) CNTs have been directly attached onto the individual fibers by different techniques: (a) direct growth of CNTs on the fibers; (b) electrophoretic deposition; and (c) spraying. These studies have demonstrated that CNTs offer intra and interlaminar reinforcement, improving delamination resistance and out-of-plane properties without sacrificing the in-plane performance (see [14] for a review on the subject). Meanwhile, the use of graphene as nanoreinforcement for the development of hierarchical composites has not been widely studied [17–20]. Graphene exhibits outstanding intrinsic properties, and has been shown to be an effective reinforcement of composite materials [21–23]. It has some advantages over carbon nanotubes, such as lower cost, larger surface area, functional groups on its surface, and easier processing. In addition, graphene does not increase the viscosity of the resin as much as carbon nanotubes do, enabling the incorporation of higher concentrations into the system.

The objective of this study is to analyze the effect of graphene on the morphology and mechanical properties of carbon fiber-reinforced epoxy composites prepared by vacuum-assisted resin infusion molding. The properties are compared to those of carbon nanotube-reinforced composites. Two routes were used for producing the hierarchical composites: (i) adding graphene directly to the resin by calender mixing, and (ii) depositing the graphene onto the carbon fiber surface by spraying.

2. Materials and Methods

The resin used in this study is a commercially available, two-component system based in an epoxy MGS RIM 135 (Hexion Inc., Columbus, OH, USA) and a curing agent composed of two amine hardeners, RIM H137 and RIM H134, in a 80:20 ratio. The resin and the hardener must be thoroughly mixed at a specified ratio of 100:30 in parts by weight. It is a very low viscosity system, especially suited for infusion processes. According to the supplier's specifications, the curing reaction is carried out at 80 °C for 120 min, and followed by a post-curing step at 130 °C for 90 min.

As nanoparticle, we selected commercial multi-wall carbon nanotubes with an average diameter of 9.5 nm, average length of 1.5 μm and a specific surface area of 250–300 m^2g^{-1}, supplied by Nanocyl with the tradename of NC7000 (Nanocyl SA, Sambreville, Belgium), and an in-house synthetized thermally reduced graphene oxide (TRGO). The graphite oxide (GO) was prepared from commercial graphite following a previously described modified Hummers' method [24,25]. Briefly, concentrated H_2SO_4 (360 mL) was added to a mixture of graphite (7.5 g) and $NaNO_3$ (7.5 g) and followed by a careful addition of $KMnO_4$ (45 g). The solution was heated to 35 °C and stirred for 3 h. Finally, 3% H_2O_2 (1.5 L) was slowly added to the reactor and stirred for 30 min and, subsequently, centrifuged (4000 rpm for 10 min). The remaining solid material was washed with deionized water, centrifuged until neutral pH and vacuum dried. The TRGOs were obtained by thermal exfoliation/reduction from GO at 1000 °C, as described elsewhere [26,27]. Unidirectional (UD) carbon fiber tape of 12 k, density of 340 gr/m^2, thickness of 0.45 mm, and width of 120 mm, was supplied by INP96 (INP 96 SL, Madrid, Spain).

The hierarchical composites were prepared using a vacuum-assisted resin infusion molding (VARIM), in which, two routes for incorporating the carbon nanoparticles were evaluated:

(i) adding the nanoparticles directly to the resin (polymer nanocomposite). The dispersion of the nanoparticles in the epoxy resin was carried out by means of a three-roll calender (EXAKT 80E, EXAKT Technologies, Inc. Oklahoma City, OK, USA), under the processing conditions described elsewhere [27]. The materials were prepared at two TRGO contents: 0.5 and 1 wt.% in relation to the epoxy resin content. In the case of MWCNTs, only 0.5 wt.% was added, because the viscosity increased dramatically. The hardener was then added in a stoichiometric ratio, and the mixture was degassed for 1 h at room temperature under vacuum.

(ii) depositing the graphene onto the carbon fiber surface by spraying (surface modified fiber). A dispersion of the nanoparticles in ethanol, at the desired concentration, was sprayed onto the surface of the fibers to add 0.5 and 1.0 wt.% of nanoparticles in the laminates. Then, the fibers are dried in an oven at 70 °C for 30 min to remove the solvent.

All hierarchical composites consist of 6 carbon fiber laminates of 250 mm length, 120 mm width, and 2 mm thickness. The carbon fiber content in the laminate is about of 75 wt.%. The fibers are arranged unidirectionally and the infusion is made in the direction of the fiber. The produced composites are described in Table 1, and the nomenclature used is: method of incorporation of the nanoparticle: (C: calender, and S: Spray); type of nanoparticle: (G: graphene, and CNT: carbon nanotube) and nanoparticle concentration in the composite: 0.5 and 1 wt.%.

Table 1. Mechanical properties of hierarchical composites.

Laminate	Tensile Tests						ILSS, τ_{13}, MPa
	0°		90°		±45°		
	Young's Modulus, E_1, GPa	Maximum Strength, MPa	Young's Modulus, E_2, GPa	Maximum Strength, MPa	Modulus, G_{12}, MPa	Strength, MPa	
Cblank	128.2 ± 4.2	1630.7 ± 58.8	9.7 ± 0.6	45.6 ± 0.9	4249.6 ± 109.7	32.3 ± 0.3	52.2 ± 1.6
CG05	126.8 ± 4.8	1726.0 ± 20.4	8.6 ± 0.5	41.5 ± 1.6	4458.6 ± 112.4	28.2 ± 0.2	52.6 ± 1.2
CG1	126.1 ± 3.2	1715.4 ± 49.6	9.3 ± 0.2	48.6 ± 1.1	5077.9 ± 123.7	33.1 ± 0.5	55.2 ± 1.1
CCNT05	134.0 ± 2.4	1723.5 ± 46.1	8.8 ± 0.2	48.0 ± 0.9	4938.2 ± 63.8	32.0 ± 0.2	57.4 ± 1.0
SG05	120.7 ± 4.0	1562.5 ± 73.2	9.6 ± 0.2	46.0 ± 1.5	4937.0 ± 88.7	31.3 ± 0.2	57.7 ± 1.5
SG1	125.2 ± 1.6	1660.1 ± 73.2	8.8 ± 0.3	44.8 ± 0.5	4257.3 ± 71.4	29.0 ± 0.4	54.2 ± 2.2
SCNT05	127.5 ± 6.5	1640.0 ± 49.3	9.4 ± 0.5	48.9 ± 0.5	4648.0 ± 151.1	31.2 ± 0.3	60.3 ± 1.4
SCNT1	119.8 ± 5.7	1514.0 ± 36.9	8.7 ± 0.2	48.0 ± 1.5	4286.4 ± 82.1	28.2 ± 0.2	56.5 ± 1.3

Mechanical testing was done to determine the tensile properties of the composites measured in three orientations with respect to fiber direction, 0° and 90° according to American Society for Testing and Materials (ASTM) D3039 and ±45° according to ASTM D3518. The interlaminar shear strength (ILSS) was also evaluated by short beam 3-point bending according to ASTM D2344. At least six laminates of each composite were tested.

Carbon fibers surface and composite fracture surfaces were observed using a Philips XL30 (FEI SA, Hillsboro, OR, USA) environmental scanning electron microscope (ESEM) at 15 kV.

3. Results and Discussion

Figure 1 shows the surface of the carbon fibers modified by deposition of carbon nanoparticles. The spraying of the CNT dispersion on the fibers results in a matt black color more intense than graphene. In addition, CNTs adhere better to the surface of the fibers, and the laboratory paper is hardly stained by simple contact.

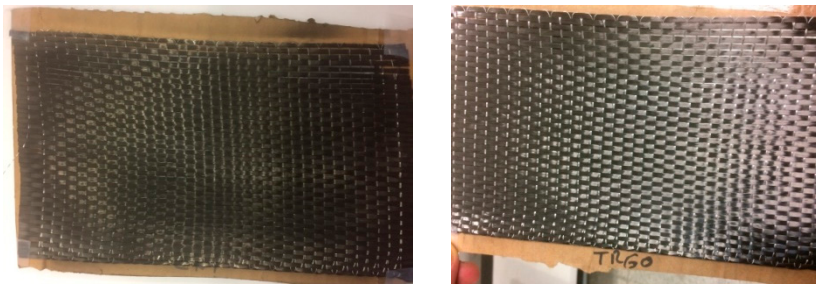

Figure 1. Surface modified carbon fiber by spraying of carbon nanoparticles: multi-walled carbon nanotubes (MWCNTs, left) and thermally reduced graphene oxide (TRGO, right).

The carbon fiber surface shows no damage from ethanol spraying, as shown by scanning electron microscopy (Figure 2). On the other hand, a homogeneous distribution of both nanoparticles is observed along the surface of the fibers. In the case of MWCNTs, a larger population of nanoparticles can be seen, interacting between adjacent fibers (Figure 2, middle).

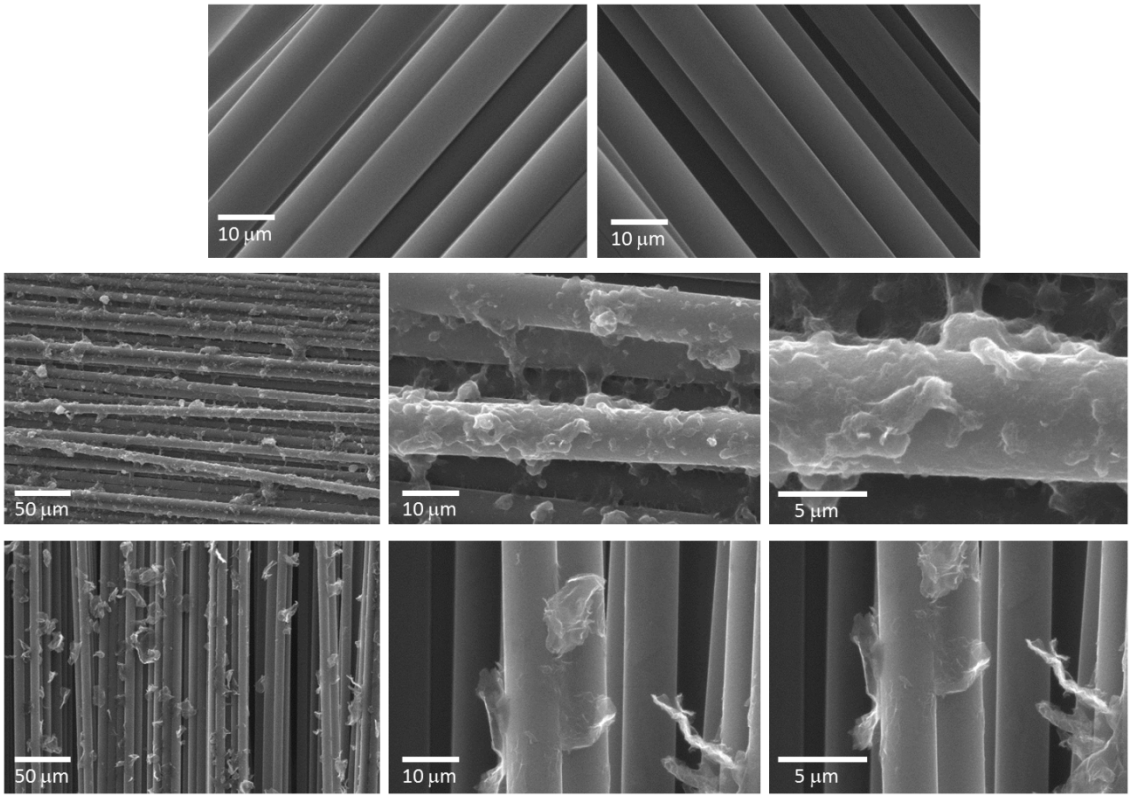

Figure 2. Scanning electron microscopy (SEM) images of carbon fiber surfaces: original fiber (top left), spraying only with ethanol (top right), spraying with CNT dispersion (middle), and spraying with graphene dispersion (bottom).

The tensile properties of the laminates in longitudinal (0°) and transversal (90°) direction to the fiber are shown in Table 1. UD-CFRPs exhibit high anisotropy, which is clearly observed in a higher modulus and strength in the fiber direction. The mechanical properties measured at 0° show a fiber-dominated behavior and the failure in the laminate is induced by its own fracture. Therefore, the effect of the nanoparticles is practically negligible, and no statistically significant differences are observed. Similar results have been observed by other authors [28–30], and even some [31] have reported a deterioration of the mechanical properties of the laminate through the addition of CNTs, due to a higher stiffness of the resin, which causes an increase in the stress around the broken fibers. Also, CNTs tend to form agglomerates, which act as microstructural defects, responsible for the appearance of premature failures in the material [30].

The tensile properties of the 90° laminates with respect to the direction of the fiber do not show significant variations by the addition of the nanoparticles. We observed only a slight increase of about 8% in the tensile strength. Similar results were observed by other authors [30–32], although in these studies, they observed an increase in ductility in the presence of nanoparticles. In transversal loads, the failure of the material is initiated in the resin itself or in the fiber–matrix interface. The authors suggested that CNTs could interfere with the failure mechanism, such as bridging, slip-through or partial debonding [30].

SEM images of the fracture surface show a good fiber–matrix interaction and no areas of dry fibers, without resin, are found (Figure 3).

For the orientation of the fiber at ± 45°, the applied load is distributed between the fiber and the matrix. The carbon nanoparticles have a minor effect on the shear stress of the laminate (Table 1); however, they have a clear reinforcing effect on the shear modulus, G_{12}. All laminates reinforced with carbon nanoparticles improve the shear modulus, achieving improvements of up to 20%. The reinforcing effect of the carbon nanoparticles depends on the method used for their

incorporation. When mixed directly with the resin by calender, the reinforcing effect of graphene gradually increases with concentration. Unfortunately, this effect cannot be corroborated for CNTs, as the viscosity of the resin at 1 wt.% increased dramatically and hindered the infusion. At the same nanoparticle concentration, 0.5 wt.%, CNTs have a more reinforcing effect than graphene. However, when spraying is used, a different behavior is observed. The highest modulus is obtained with 0.5 wt.% of nanoparticle, decreasing at higher concentrations.

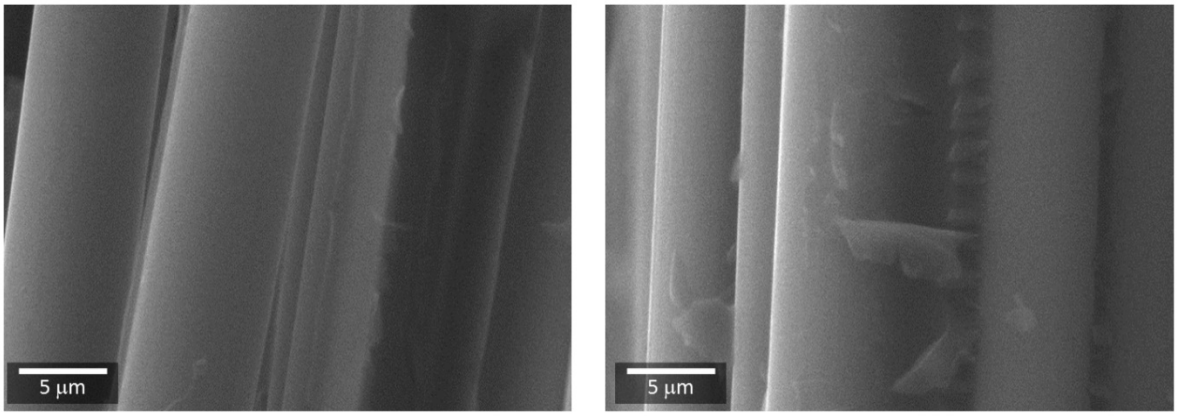

Figure 3. Scanning electron microscopy (SEM) images of the fracture surface of the laminates.

It can be concluded that, in the calender mixing method, the optimal concentration of nanoparticles is limited by the increase in the viscosity of the resin; whereas in the spraying route, the limitation is given by the formation of agglomerates on the surface of the fiber. However, it would be of interest to analyze a wider range of concentrations, which would establish the optimal nanoparticle concentration in the hierarchical composite.

One of the main limitations of continuous carbon fiber composites is their low interlaminar shear strength (ILSS), due to a poor epoxy/fiber interaction. In the three-point bending tests on a short beam, the failure is expected to occur only by shear; however, it is a complex method and other failure mechanisms such as tensile or compression may occur.

Figure 4 shows a representative stress-strain curve of the studied materials. A clear increase in load is observed at low deformations, then, it remains constant with the deformation, until it suffers a small drop in the value of the stress at higher deformations. This type of curve indicates that in addition to the interlaminar shear failure, there are other failure mechanisms that contribute to the breakage of the material, such as the appearance of microcracks in the resin (Figure 5). Similar morphology is observed for all laminates.

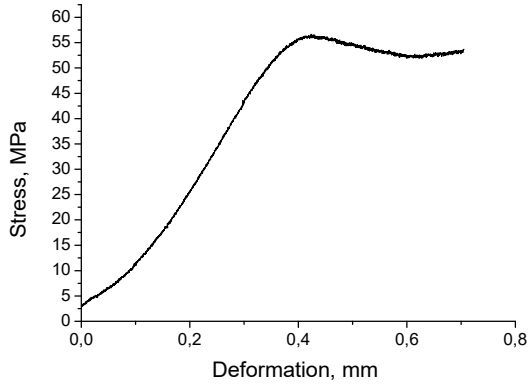

Figure 4. Typical curve of interlaminar shear strength (ILSS) tests.

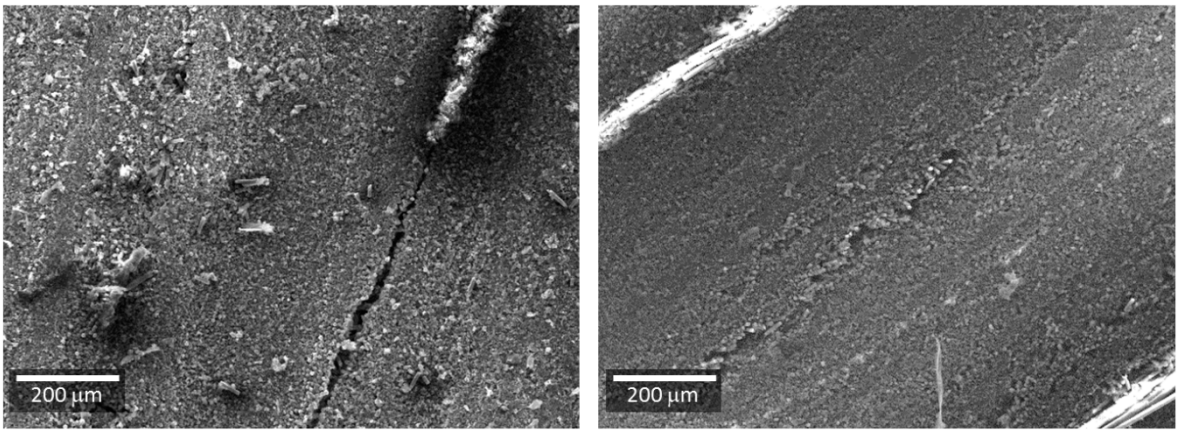

Figure 5. Scanning electron microscopy (SEM) images of failure modes in short-beam tests (**left**) and microcracks in the resin (**right**).

All hierarchical composite materials show higher interlaminar strength relative to the unreinforced composite, reaching increases of more than 15% (Table 1). This increase in the value of the resistance can be attributed to a larger contact area between the carbon fiber and the matrix due to the presence of nanoparticles. This effect is more significant when carbon nanotubes were used as nanoreinforcement, probably due to the larger population of nanoparticles on the surface of the fibers.

As noted above, there is a clear difference in the optimal concentration of nanoparticles depending on the incorporation method. The interlaminar strength gradually increases with the nanoparticle content when using the calender mixing. While in the spraying procedure, the highest strength is obtained at concentrations of 0.5 wt.% for both nanoparticles, decreasing with increasing concentration. On the other hand, although the differences are not very significant, it does seem that the laminates prepared with the fibers modified superficially by spraying show a greater ILSS in comparison with those prepared by mixing in the calender. This improvement is similar to the results reported by other authors for hierarchical composites with CNTs [33–36].

4. Conclusions

Calender mixing and spraying have been shown to be two simple and scalable methods for manufacturing hierarchical composites. The surface modification of fibers by spray enables the incorporation of higher concentration of nanoparticles in the composite, while in calender mixing, the limitation is given by the increase in viscosity of the resin. A different trend is observed between the methods of incorporating the carbon nanoparticles; in the laminates prepared by calender mixing, the mechanical properties gradually increase with the nanoparticle concentration, while in sprayed laminates, the best properties are achieved at lower concentrations, probably due to the formation of agglomerates on the surface of the fibers at higher concentrations.

Although the dispersion of graphene is easier to infuse since the viscosity of the resin is lower, both carbon nanoparticles show a similar behavior on the mechanical properties of the laminate. The fiber-dominated in-plane performances are not significantly affected by incorporating carbon nanoparticles, but do have a positive effect on through-thickness properties.

There are critical issues that need to be optimized, as the control of the dispersion of nanoparticles, the viscosity of the resin, the presence of functional groups on the nanoparticle surface, or new routes for incorporating of nanoparticles.

Author Contributions: J.M.V.-M. and R.S.-H. developed the incorporation of carbon nanoparticles; E.S.-H. manufactured the hierarchical composites; J.V. carried out the mechanical properties tests; R.V. carried out the morphological characterization and the writing, review and editing of the manuscript; and M.A.L.-M. participated in the writing, review and editing of the manuscript.

Funding: This research was funded by the Spanish Ministerio de Economía y Competitividad (MINECO), grant number MAT2016-81138-R.

Conflicts of Interest: The authors declare no conflict of interest.

References

1. Mallick, P.K. *Fiber-Reinforced Composites. Materials, Manufacturing and Design*, 3rd ed.; CRC Press: Boca Raton, FL, USA, 2008.
2. Jain, R.; Lee, L. *Fiber Reinforced Polymer (FRP) Composites for Infrastructure Applications*; Springer: Berlin/Heidelberg, Germany, 2012.
3. Bai, J. *Advanced Fibre-Reinforced Polymer (FRP) Composites for Structural Applications*; Woodhead Publishing: Cambridge, UK, 2013.
4. Ozgur Seydibeyoglu, M.; Mohanty, A.K.; Misra, M. *Fiber Technology for Fiber-Reinforced Composites*; Woodhead Publishing: Cambridge, UK, 2017.
5. Borri, A.; Castori, G.; Corradi, M.; Speranzini, E. Durability analysis for FRP and SRG composites in civil applications. *Key Eng. Mater.* **2015**, *624*, 421–428. [CrossRef]
6. Corradi, M.; Borri, A.; Righetti, L.; Speranzini, E. Uncertainty analysis of FRP reinforced timber beams. *Compos. Part B* **2017**, *113*, 174–184. [CrossRef]
7. Corradi, M.; Borri, A.; Castori, G.; Speranzini, E. Fully reversible reinforcement of softwood beams with unbounded composite plates. *Compos. Struct.* **2016**, *149*, 54–68. [CrossRef]
8. Liu, L.; Jia, C.; He, J.; Zhao, F.; Fan, D.; Xing, L.; Wang, M.; Wang, F.; Jiang, Z.; Huang, Y. Interfacial characterization, control and modification of carbon fiber reinforced polymer composites. *Compos. Sci. Technol.* **2015**, *121*, 56–72. [CrossRef]
9. Tong, L.; Mouritz, A.P.; Bannister, M.K. *3D Fibre Reinforced Polymer Composites*; Elsevier: Amsterdam, The Netherlands, 2002.
10. Vautard, F.; Ozcan, S.; Meyer, H. Properties of thermo-chemically Surface treated carbon fibers and of their epoxy and vinyl ester composites. *Compos. Part A* **2012**, *43*, 1120–1133. [CrossRef]
11. Yuan, H.; Wang, C.G.; Zhang, S.; Lin, X. Effect of surface modification on carbon fibre and its reinforced phenolic matrix composite. *Appl. Surf. Sci.* **2012**, *259*, 288–293. [CrossRef]
12. Sharma, M.; Gao, S.L.; Mader, E.; Sharma, H.; Wei, L.Y.; Bijwe, J. Carbon fiber surfaces and composite interphases. *Compos. Sci. Technol.* **2014**, *102*, 35–50. [CrossRef]
13. Major, L.; Janusz, M.; Kot, M.; Lackner, J.M.; Major, B. Development and complex characterization of bio-tribological Cr/CrNplus A-C:H (Doped Cr) nano-multilayer protective coatings for carbon fibre composite materials. *RSC Adv.* **2015**, *5*, 9405–9415. [CrossRef]
14. Qian, H.; Greenhalgh, E.S.; Shaffer, M.S.P.; Bismarck, A. Carbon nanofiber –base hierarchical composites: A review. *J. Mater. Chem.* **2010**, *20*, 4751–4762. [CrossRef]
15. Karger-Kocsis, J.; Mahmood, H.; Pegoretti, A. Recent advances in fiber/matrix interphase engineering for polymer composites. *Prog. Mater. Sci.* **2010**, *73*, 1–43. [CrossRef]
16. Ghasemi-Nejhad, M.N. Hierarchical multifunctional nanocomposites. *SPIE* **2014**, *9058*, 905801–905816.
17. Qin, W.; Vautard, F.; Drzal, L.T.; Yu, J. Mechanical and electrical properties of carbon fiber composites with incorporation of graphene nanoplatelets at the fiber–matrix interphase. *Compos. Part B* **2015**, *69*, 335–341. [CrossRef]
18. Zhang, R.L.; Gao, B.; Ma, Q.H.; Zhang, J.; Cui, H.Z.; Liu, L. Directly grafting graphene oxide onto carbon fiber and the effect on the mechanical properties of carbon fiber composites. *Mater. Des.* **2016**, *93*, 364–369. [CrossRef]
19. Wang, C.; Li, J.; Yu, J.; Sun, S.; Li, X.; Xie, F.; Jiang, B.; Wu, G. Grafting of size-controlled graphene oxide sheets onto carbon fiber for reinforcement of carbon fiber/epoxy composite interfacial strength. *Compos. Part A* **2015**, *101*, 511–520. [CrossRef]
20. Liu, L.; Yan, F.; Li, M.; Zhang, M.; Xiao, L.; Shang, L.; Ao, Y. Improving interfacial properties of hierarchical reinforcement carbon fibers modified by graphene oxide with different bonding types. *Compos. Part A* **2018**, *107*, 616–625. [CrossRef]
21. Kim, H.; Abdala, A.A.; Macosko, C.W. Graphene/polymer nanocomposites. *Macromolecules* **2010**, *43*, 6515–6530. [CrossRef]

22. Potts, J.R.; Dreyer, D.R.; Bielawski, C.W.; Ruoff, R.S. Graphene-based polymer nanocomposites. *Polymer* **2011**, *52*, 5–25. [CrossRef]
23. Verdejo, R.; Bernal, M.M.; Romasanta, L.J.; Lopez-Manchado, M.A. Graphene filled polymer nanocomposites. *J. Mater. Chem.* **2011**, *21*, 3301–3310. [CrossRef]
24. Botas, C.; Álvarez, P.; Blanco, C.; Santamaría, R.; Granda, M.; Ares, P.; Rodríguez-Reinoso, F.; Menéndez, R. The Effect of the parent graphite on the structure of graphene oxide. *Carbon* **2012**, *50*, 275–282. [CrossRef]
25. Botas, C.; Álvarez, P.; Blanco, P.; Granda, M.; Blanco, C.; Santamaría, R.; Romasanta, L.J.; Verdejo, R.; López-Manchado, M.A.; Menéndez, R. Graphene materials with different structures prepared from the same graphite by the Hummers and Brodie methods. *Carbon* **2013**, *65*, 156–164. [CrossRef]
26. Vazquez-Moreno, J.M.; Yuste-Sanchez, V.; Sanchez-Hidalgo, R.; Verdejo, R.; Lopez-Manchado, M.A.; Fernández-García, L.; Blanco, C.; Menéndez, R. Customizing thermally-reduced graphene oxides for electrically conductive or mechanical reinforced epoxy nanocomposites. *Eur. Polym. J.* **2017**, *93*, 1–7. [CrossRef]
27. Sánchez-Hidalgo, R.; Yuste-Sanchez, V.; Verdejo, R.; Blanco, C.; Lopez-Manchado, M.A.; Menéndez, R. Main structural features of graphene materials controlling the transport properties of epoxy resin-based composites. *Eur. Polym. J.* **2018**, *101*, 56–65. [CrossRef]
28. Iwahori, Y.; Ishiwata, S.; Sumizawa, T.; Ishikawa, T. Mechanical properties improvements in two-phase and three-phase composites using carbon nano-fiber dispersed resin. *Compos. Part A* **2005**, *36*, 1430–1439. [CrossRef]
29. Qiu, J.; Zhang, C.; Wang, B.; Liang, R. Carbon nanotube integrated multifunctional multiscale composites. *Nanotechnology* **2007**, *18*, 275708. [CrossRef]
30. Godara, A.; Mezzo, L.; Luizi, F.; Warrier, A.; Lomov, S.V.; van Vuure, A.W.; Gorbatikh, L.; Moldenaers, P.; Verpoest, I. Influence of carbon nanotube reinforcement on the processing and the mechanical behaviour of carbon fiber/epoxy composites. *Carbon* **2009**, *47*, 2914–2923. [CrossRef]
31. Sánchez-Campo, M.; Jiménez-Suárez, A.; Ureña, A. Effect of the carbon nanotube functionalization on flexural properties of multiscale carbon fiber/epoxy composites manufactured by VARIM. *Compos. Part B* **2013**, *45*, 1613–1619. [CrossRef]
32. Ci, L.; Bai, J. The reinforcement role of carbon nanotubes in epoxy composites with different matrix stiffness. *Compos. Sci. Technol.* **2006**, *66*, 599–603. [CrossRef]
33. Chandrasekaran, V.C.S.; Advani, S.G.; Santare, M.H. Role of processing on interlaminar shear strength enhancement of epoxy/glass fiber/multi-walled carbon nanotube hybrid composites. *Carbon* **2010**, *48*, 3692–3699. [CrossRef]
34. Wu, G.; Ma, L.; Liu, L.; Wang, Y.; Xie, F.; Zhong, Z.; Zhao, M.; Jiang, B.; Huang, Y. Interfacially reinforced methylphenylsilicone resin composites by chemically grafting multiwall carbon nanotubes onto carbon fibers. *Compos. Part B* **2015**, *82*, 50–58. [CrossRef]
35. Rong, H.; Dahmen, K.H.; Garmestani, H.; Yu, M.; Jacob, K.I. Comparison of chemical vapor deposition and chemical grafting for improving the mechanical properties of carbon fiber/epoxy composites with multi-wall carbon nanotubes. *J. Mater. Sci.* **2013**, *48*, 4834–4842. [CrossRef]
36. Fan, W.; Wang, Y.; Wang, C.; Chen, J.; Wang, Q.; Yuan, Y.; Niu, F. High efficient preparation of carbon nanotube-grafted carbon fibers with the improved tensile strength. *Appl. Surf. Sci.* **2016**, *364*, 539–551. [CrossRef]